

Properties of the defect modes in 1D lossy photonic crystals containing two types of negative-index-material defects

A. Aghajamali ^{1,2*} M. Hayati ^{3†}, C.-J. Wu ^{4‡}, and M. Barati ^{2§}

¹ *Young Researchers Club,*

Science and Research Branch,

Islamic Azad University, Fars, Iran

² *Department of Physics,*

Science and Research Branch,

Islamic Azad University, Fars, Iran

³ *Department of Physics, Marvdasht Branch,*

Islamic Azad University, Marvdasht, Iran

⁴ *Institute of Electro-Optical Science and Technology,*

National Taiwan Normal University,

Taipei 116, Taiwan, R.O.C.

Abstract

In this paper, the characteristic matrix method is employed to theoretically investigate the propagation of electromagnetic waves through one-dimensional defective lossy photonic crystals (PCs) composed of negative index materials (NIMs) and positive index materials (PIMs). We consider symmetric and asymmetric geometric structures with two different types of NIM defect layers at the center of the structure. The effects of the polarization and the angle of incidence on the defect modes in the transmission spectra of both structures are investigated. The results show that the number of the defect modes within the photonic band gap (PBG) depends on the type of the NIM defect layer and is independent of the geometrical structure. Moreover, it is shown that the defect mode frequency increases as the angle of incidence increases. This property is also independent of the geometry of the structure. The results can lead to designing new types of narrowband and multichannel transmission filters.

* email address: alireza.aghajamali@fsriau.ac.ir

† email address: mjhayati@yahoo.com

‡ email address: jasperwu@ntnu.edu.tw

§ email address: barati@susc.ac.ir

I. INTRODUCTION

Over the past two and half decades, a new class of material called photonic crystals (PCs) has emerged. The PCs originate from theoretical work of Yablonovitch, and John's experimental work, which were published almost simultaneously in 1987 [1, 2]. The PCs are artificial dielectric or metallic structures in which the refractive index changes periodically in space. This kind of periodic structure affects the propagation of electromagnetic waves in the similar way as the periodic potential in a semiconductor crystal affects the electron motion by defining allowed and forbidden electronic energy bands. Whether or not photons propagate through PC structures depends on their frequency. Frequencies that are allowed to travel are known as modes, and groups of allowed modes form bands. Disallowed bands of frequencies are called photonic band gaps (PBGs) [3, 4]. These PBGs are also called the Bragg gaps because they originate from the Bragg scattering in the periodic structure. The properties of PBGs in one-dimensional (1D) PCs have been proven to play an important role in some potential applications such as photonic devices, optical filters, resonance cavities, laser applications, high reflecting omnidirectional mirrors, and the optoelectronic circuits [5-8].

By breaking the periodicity of the conventional PC structure, we will have a defective crystal. This can be performed by changing physical parameters, such as changing the thickness of one of the layer, adding another medium to the structure, or removing a layer from PCs [9-14]. By introducing a layer with different optical properties, localized defect modes, which are also called resonant transmission peaks, can be generated within the PBG due to the change of the interference behavior of light [14, 15], very similar to the defect states that are generated in the forbidden band of doped semiconductors. Upon prediction of the existence of materials with negative refractive index (NRI) in 1968 by Veselago [16], such materials, which have negative permittivity and permeability simultaneously, have received extensive attention for their very unusual electromagnetic properties. Negative refractive index materials, or simply negative index materials (NIMs), are now also known as metamaterials. Recently, with the possibility of producing metamaterials, PCs with metamaterials, called metamaterial photonic crystals (MPCs) have been made.

In several papers the properties of the defect modes in different 1D conventional PC and 1D MPC structures have been investigated by introducing positive or negative indices defects [17-35]. Following the interesting report by Wu et al. [23] on the properties of the defect modes in 1D PCs with symmetric and asymmetric geometric structures, here we investigate the properties of the defect modes in the transmission spectra of 1D defective symmetric and asymmetric lossy

MPCs which are composed of negative refractive index material defect layer at the center of the crystal. The outline of this paper is as follows. In Section 2, two geometric MPC structures, the permittivity and permeability of two types of NIMs, and also the characteristic matrix method and its formulation are presented. The numerical results and discussions are given in Section 3, and the conclusion is presented in Section 4.

II. MPC STRUCTURE AND CHARACTERISTIC MATRIX METHOD

The 1D defective MPCs, which are constituted by alternative layers of NIM and positive index material (PIM), under study with asymmetric and symmetric structures in air with a defect layer at the center of the structures are shown in Figures 1(a) and 1(b), respectively, where NIMs are dispersive and dissipative. We assume that layers A and C (defect layer) are NIMs, and layer B is a PIM. N is the number of the lattice period, and also d_i , ε_i , and μ_i ($i = A, B, C$) are thickness, permittivity and permeability of the layers, respectively.

The calculations are performed using the characteristic matrix method [36], which is the most effective technique to analyze the transmission properties of PCs. The characteristic matrix for $(AB)^{N/2}C(AB)^{N/2}$, and symmetric $(AB)^{N/2}C(BA)^{N/2}$ structures, are given by:
 $M[d] = (M_A M_B)^{N/2} M_C (M_A M_B)^{N/2}$, and $M[d] = (M_A M_B)^{N/2} M_C (M_B M_A)^{N/2}$,
where M_A , M_B and M_C are the characteristic matrices of layers A , B , and C . The characteristic matrix M_i for TE wave is given by [36]:

$$M_i = \begin{bmatrix} \cos \gamma_i & \frac{-i}{p_i} \sin \gamma_i \\ -i p_i \sin \gamma_i & \cos \gamma_i \end{bmatrix} \quad (1)$$

where, $\gamma_i = (\omega/c) n_i d_i \cos \theta_i$, c is speed of light in vacuum, θ_i is the ray angle inside the layer i with refractive index n_i , $p_i = \sqrt{\varepsilon_i / \mu_i} \cos \theta_i$, and $\cos \theta_i = \sqrt{1 - (n_0^2 \sin^2 \theta_0 / n_i^2)}$, in which n_0 is the refractive index of the environment wherein the incidence wave tends to enter the structure. The refractive index is given as $n_i = \pm \sqrt{\varepsilon_i \mu_i}$ [31, 37], where the positive and the negative signs are assigned for the PIM and NIM layers, respectively.

The final characteristic matrix for an N period structure is given by:

$$[M(d)]^N = \prod_{i=1}^N M_i \equiv \begin{pmatrix} m_{11} & m_{12} \\ m_{21} & m_{22} \end{pmatrix}, \quad (2)$$

where $m_{i,j}(i, j = 1, 2)$ are the matrix elements of $[M(d)]^N$. The transmission coefficient of the

multilayer is calculated by:

$$t = \frac{2 p_0}{(m_{11} + m_{12} p_s) p_0 + (m_{21} + m_{22} p_s)}. \quad (3)$$

In this equation, $p_0 = n_0 / \cos \theta_0$ and $p_s = n_s / \cos \theta_s$, with n_s being the refractive index of the environment where the wave leaves the crystal with angle θ_s . The transmissivity of the multilayer is given by $T = (p_s/p_0)|t|^2$. The transmissivity of the multilayer for TM waves can be obtained by using these previous expressions with $p_i = \sqrt{\mu_i/\varepsilon_i} \cos \theta_i$, $p_0 = \cos \theta_0/n_0$, and $p_s = \cos \theta_s/n_s$.

As mentioned before, our study is based on two different types of NIMs. The permittivity and permeability of type-I NIM layer with negative refracting index in the microwave region are complex, and are defined as [38, 39],

$$\varepsilon(f) = 1 + \frac{5^2}{0.9^2 - f^2 - i\gamma f} + \frac{10^2}{11.5^2 - f^2 - i\gamma f} \quad (4)$$

$$\mu(f) = 1 + \frac{3^2}{0.902^2 - f^2 - i\gamma f} \quad (5)$$

where f and γ are frequency and damping frequency in GHz, respectively. As mentioned in [39], for $f < 3.13$ GHz, the real parts of the permittivity and permeability, ε' and μ' , are simultaneously negative (double-negative material). For $3.13 < f < 3.78$ GHz, $\varepsilon' < 0$, but $\mu' > 0$ (single-negative material extending to the epsilon-negative material), and also for $f > 3.78$ GHz, both ε' and μ' are positive (double-positive material). For type-II NIM layer, we use the Drude model [40] to describe the complex permittivity and permeability, with the results

$$\varepsilon(f) = 1 - \frac{100}{f^2 - i\gamma f} \quad (6)$$

$$\mu(f) = 1.44 - \frac{100}{f^2 - i\gamma f}. \quad (7)$$

Similarly, f and γ are respectively frequency and damping frequency, given in GHz. For $f < 8.33$ GHz, both ε' and μ' , the real parts of the permittivity and permeability, are negative (double-negative material), and for $8.33 < f < 10$ GHz, $\varepsilon' > 0$, but $\mu' < 0$ (mu-negative material).

III. NUMERICAL RESULTS AND DISCUSSION

Based on the theoretical model described in previous section, the transmission spectrum of the lossy defective PC with a NIM defect layer at the center is calculated. The calculations are carried out in the region where the real parts of the permittivity and permeability of two types of NIM

layers (layers A , and C), ε' and μ' , are simultaneously negative where the zero- \bar{n} gap will appear [38, 39, 41, 42]. Equations (4) and (5), type-I NIM, are used for the permittivity and permeability of layer A . PIM layer (layer B) is assumed to be the vacuum layer with $n_B = 1$. The thickness of layers A , B , and C are respectively chosen as $d_A = 6$ mm, $d_B = 12$ mm, and $d_C = 24$ mm. Also, the total number of the lattice period is selected to be $N = 16$ [39].

In the first part, we use equations (4) and (5), type-I NIM, for the permittivity and the permeability of NIM defect layer (layer C) exactly like layer A , and the transmission spectra of two different asymmetric and symmetric geometric structures for both polarizations are investigated. First of all, the transmission spectra of TE and TM polarized waves for the asymmetric structure at various angles of incidence and for $\gamma = 0.2 \times 10^{-3}$ GHz are shown in Figures 2 and 3. As it is seen, a single resonant peak appears within the PBG, which corresponds to the type-I NIM defect layer. This is in line with the report by Wu et al. [23] for the defect modes in 1D PCs with PIMs where only one defect mode for the asymmetric structure has been observed. In addition, the figures show that as the angle of incidence increases, the peak height of the defect mode decreases for TE waves and increases for TM waves. Moreover, for both polarizations the frequency of the defect mode is shifted to the higher frequency as the angle increases.

In Figures 4 and 5 we have plotted the frequency-dependent transmittance for the symmetric structure in TE and TM waves at four different angles of incidence. As it is observed in these figures, similar to the asymmetric structure, there is a single defect mode within the band gap again. This is in sharp contrast to the work by Wu et al. [23] for the defect modes in 1D symmetric PC with PIMs where there are two defect modes. It is also worth mentioning that the number of defect modes appearing with type-I NIM defect layer does not depend on the geometric structure, polarization, and angle of the incidence wave.

In more detail, as shown in Figure 6, the frequency of defect mode versus the angle of incidence for asymmetric (Figure 6(a)) and symmetric (Figure 6(b)) structures have been respectively plotted. As we mentioned earlier, only one defect mode appears in both asymmetric and symmetric structures. Additionally, as seen from the figures, in the asymmetric structure the defect modes appear in higher frequencies compared to the symmetric one. Another feature in Figure 6 which is worth mentioning is the frequency of the defect mode, which, in TE waves, remains nearly unchanged in both geometric structures as the angle of incidence increases. However, in TM waves, the frequency increases as the angle of incidence increases. In addition, this increase in symmetric structure is higher than that of asymmetric one.

In the second part, properties of the defect mode of both geometric structures with another type

of NIM defect layer at the center (type-II NIM), which was described in Section 2, are investigated. The asymmetric and symmetric structures which were used before are modified by replacing type-II NIM defect layer (layer C), in which the permittivity and permeability follow the equations (6) and (7). The other parameters are kept the same as the first part.

In Figures 7 and 8, we have respectively plotted the transmission spectra of TE and TM waves for the asymmetric structure at various angles of incidence, when the loss factors of two types of NIMs, layer A and C , are equal to $\gamma = 0.2 \times 10^{-3}$ GHz. We observe that there are three defect modes for both TE and TM waves, as identified by numbers 1, 2, and 3, respectively. Additionally, the transmission spectra of TE and TM waves for the symmetric structure have been plotted in Figures 9 and 10, respectively. In the symmetric structure, similar to the asymmetric one, there are three defect modes again. It can be seen from Figures 7 to 10 that the frequencies of the defect modes are shifted to the higher frequency as the incidence angle increases. Besides, these figures show that for both asymmetric and symmetric structures, three defect modes appear, which are independent of the geometry of the structure. To the contrary, as mentioned by Wu et al. [23], in the conventional PCs case for a PIM defect layer, the symmetric geometric structure shows two defect modes and the asymmetric one shows one defect mode.

In more detail, we have plotted the defect mode frequency versus angle of incidence for both asymmetric (Figure 11(a)) and symmetric (Figure 11(b)) structures. As seen from these figures, in TE waves for both geometric structures, the frequency of defect modes remains nearly unchanged with increasing the angle of incidence. On the other hand, frequency of defect modes in TM waves increases as the angle of incidence increases. Additionally, similar to the first part, in the asymmetric structure the defect modes appear in higher frequencies compared to the symmetric one. In contrast to type-I NIM defect layer, frequencies of defect modes, which increase in the asymmetric structure, are higher than that of the symmetric structure. Another feature in Figure 11 is that in the asymmetric structure, defect modes 1 and 2 disappear for angles more than 45° and 65° , respectively. Also, defect modes 1 and 2 disappear for angles more than 55° and 70° , respectively, in the symmetric structure. To the contrary, Figure 6, by comparing defect mode 3 in both geometric structures for TM waves, shows that the frequency of the defect mode in the asymmetric structure changes more than that of the symmetric one.

As we observe, in comparison to the first part, which is type-I NIM defect layer, the number of defect modes depends on the types of NIMs which are being used for the defect layer. In addition, as the figures show, for two types of NIMs, the number of defect modes does not depend on the geometric structure. This is in sharp contrast with the work done by Wu et al. [23] where the

number of defect modes depends on the asymmetric or symmetric structure.

IV. CONCLUSION

This paper has theoretically investigated the properties of defect modes coming from two types of NIMs defect layer at the center of 1D defective lossy MPCs in symmetric and asymmetric geometric structures. Our numerical results show that there exists a single defect mode inside the PBG in both asymmetric and symmetric structures for TE and TM polarized waves, when the type-I NIM defect layer is considered. On the other hand, the results show that with changing the types of NIMs in the defect layer, we observe three defect modes inside the band gap for both structures. Positions (frequencies) of the defect modes depend on the polarization of the waves and the incidence angles. As the incidence angle increases, the frequency of the defect modes moves toward higher frequencies regardless of the geometrical structures and types of NIMs defect layer. Additionally, the results of this study bring up the conclusion that the number of defect modes in 1D asymmetric and symmetric lossy PCs strongly depends on the types of NIM defect. Besides, an important result is that by using an NIM in the structure of PCs, the defect modes show different behavior from that of the PCs with only PIMs. Finally, it is worthwhile to mention that the number of defect modes does not depend on the asymmetric or symmetric structures, contrary to the work conducted by Wu et al. [23]. Detailed analysis of the defect modes in metamaterial photonic crystals with different geometric structures will certainly provide useful information for designing new types of narrowband and multichannel transmission filters.

Acknowledgments

A. Aghajamali would like to acknowledge his gratitude to P. Shams for her help and useful discussion.

References

- [1] Yablonovitch, E., "Inhibited spontaneous emission in solid-state physics and electronics," *Phys. Rev. Lett.*, Vol. 58, 2059-2062, 1987.
- [2] John, S., "Strong localization of photons in certain disordered dielectric superlattices," *Phys. Rev. Lett.*, Vol. 58, 2486-2489, 1987.

- [3] Yablonovitch, E., "Photonic band structure: the face-centered-cubic case employing nonspherical atoms," *Phys. Rev. Lett.*, Vol. 67, 2295-2298, 1991.
- [4] Joannopoulos, J.D., S.G. Johnson, J.N. Winn, and R.D. Meade, *Photonic crystals: Modeling the flow of light*, Princeton University Press, Princeton, 2008.
- [5] Gu, X., X.F. Chen, Y.P. Chen, X.L. Zheng, Y.X. Xia, and Y.L. Chen, "Narrowband multiple wavelengths filter in aperiodic optical superlattice," *Opt. Commun.*, Vol. 237, 53, 2004.
- [6] Massaoudi, S., A. de Lustrac, and I. Huynen, "Properties of metallic photonic band gap material with defect at microwave frequencies: calculation and experimental verification," *J. Electromagn. Waves Appl.*, Vol. 14, 1967-1980, 2006.
- [7] Mandal, B. and A.R. Chowdhury, "Spatial soliton scattering in a quasi phase matched quadratic media in presence of cubic nonlinearity," *J. Electromagn. Waves Appl.*, Vol. 1, 123-135, 2007.
- [8] Zheng, Q.R., B.Q. Lin, and N.C. Yuan, "Characteristics and applications of a novel compact spiral electromagnetic band-gap (EBG) structure," *J. Electromagn. Waves Appl.*, Vol. 2, 199-213, 2007.
- [9] Boedecker, G. and C. Henkel, "All frequencies effective medium theory of a photonic crystal," *Opt. Express*, Vol. 11, 1590-1595, 2003.
- [10] Schneider, G.J. and G.H. Watson, "Nonlinear optical spectroscopy in one-dimensional photonic crystals," *Appl. Phys. Lett.*, Vol. 83, 5350-5352, 2003.
- [11] Inouye, H., M. Arakawa, J.Y. Ye, T. Hattori, H. Nakatsuka, and K. Hirao, "Optical properties of a total-reflection-type one-dimensional photonic crystal," *IEEE J. Quantum Electron.*, Vol. 38, 867-871, 2002.
- [12] Mansouriu, J.A., C.J. Zapata-Rodriguez, E. Silvestre, and W.D. Furlan, "Cantor-like fractal photonic crystal waveguides," *Opt. Commun.*, Vol. 252, 46-51, 2005.
- [13] T. Hattori, "Third-order nonlinear enhancement in one-dimensional photonic crystal structure," *Jpn. J. Appl. Phys.*, Vol. 41, 1349-1353, 2002.
- [14] Smith, D.R., R. Dalichaouch, N. Kroll, S. Schultz, S.L. McCall, and P.M. Platzman, "Photonic band structure and defect in one and two dimension," *J. Opt. Soc. Am. B*, Vol. 10, 314-321, 1993.
- [15] Jiang, X.Y., D. Xiao-yu, and W. Shuang-chun, "Effects of negative index medium defect layers on the transmission properties of one-dimensional photonic crystal," *Optoelectronics Lett.*, Vol. 15, 144-147, 2007.
- [16] Veselago, V. G., "The electrodynamics of substances with simultaneously negative values of ϵ and μ ," *Sov. Phys. Usp.*, Vol. 10, 509-514, 1968.
- [17] Lotfi, E., K. Jamshidi-Ghaleh, F. Moslem, and H. Masalehdan, "Comparison of photonic crystal narrow filters with metamaterials and dielectric defects," *Eur. Phys. J. D*, Vol. 60, 369-372, 2010.
- [18] Zhu, Q. and Y. Zhang, "Defect modes and wavelength tuning of one-dimensional photonic crystal with lithium niobate," *Optik*, Vol. 120, 195-198, 2009.
- [19] Lyubchanskii, I.L., N.N. Dadoenkova, A.E. Zabolotin, Y.P. Lee, Th. Rasing, "A one-dimensional photonic crystal with a superconducting defect layer," *J. Opt. A: Pure Appl. Opt.*, Vol. 11, 114014-114017,

2009.

- [20] Ansari, N., M.M. Tehrani, and M. Ghanaatshoar, "Characterization of defect modes in one-dimensional photonic crystals: An analytic approach," *Physica B*, Vol. 404, 1181-1186, 2009.
- [21] Li, X., K. Xie, and H.M. Jiang, "Properties of defect modes in one-dimensional photonic crystals containing two nonlinear defects," *Opt. Commun.*, Vol. 282, 4292-4295, 2009.
- [22] Hung, H.C., C.J. Wu, and S.J. Chang, "A mid-infrared tunable filter in a semiconductor-dielectric photonic crystal containing a semiconductor defect," *Solid State Commun.*, Vol. 151, 1677-1680, 2011.
- [23] Wu, C.J. and Z. H. Wang, "Properties of defect modes in one-dimensional photonic crystals," *Progress In Electromagnetics Research*, Vol. 103, 169-184, 2010.
- [24] King, T.C., Y.P. Yang, Y.S. Liou, and C.J. Wu, "Tunable defect mode in a semiconductor-dielectric photonic crystal containing an extrinsic semiconductor defect," *Solid State Commun.*, Vol. 152, 2189-2192, 2012.
- [25] Hu, C.A., J.W. Liu, C.J. Wu, T.J. Yang, and S.L. Yang, "Effects of superconducting film on the defect mode in dielectric photonic crystal heterostructure," *Solid State Commun.*, Vol. 157, 54-57, 2013.
- [26] Gharaati, A. and H. Azarshab, "Characterization of defect modes in one-dimensional ternary metal-dielectric nanolayered photonic crystal," *Progress In Electromagnetics Research B*, Vol. 37, 125-141, 2012.
- [27] Zhang, W., P. Han, A. Lan, Y. Li, and X. Zhang, "Defect modes tuning of one-dimensional photonic crystals with lithium niobate and silver material defect," *Physica E*, Vol. 44, 813-815, 2012.
- [28] Aly, A.H. and H.A. Elsayed, "Defect mode properties in a one-dimensional photonic crystal," *Physica B*, Vol. 407, 120-125, 2012.
- [29] Chen, Y.H., G.Q. Liang, J.W. Dong, and H.Z. Wang, "Derivation and characterization of dispersion of defect modes in photonic band gap from stacks of positive and negative index materials," *Phys. Lett. A*, Vol. 351, 446-451, 2006.
- [30] Kang-Song, T., X. Yuan-Jiang, and W. Shuang-Chun, "Defect in photonic crystal with negative index material," *Optoelectron. Lett.*, Vol. 2, 118-121, 2006.
- [31] Jiang, H., H. Chen, H. Li, and Y. Zhang, "Omnidirectional gap and defect mode of one-dimensional photonic crystals containing negative-index materials," *Appl. Phys. Lett.*, Vol. 83, 5386-5388, 2003.
- [32] Wang, L.G., H. Chen, and S.Y. Zhu, "Omnidirectional gap and defect mode of one-dimensional photonic crystals with single-negative materials," *Phys. Rev. B*, Vol. 70, 245102-245107, 2004.
- [33] Xu, Q., K. Xie, H. Yang, and J. Tang, "Periodic defect modes of one-dimensional crystals containing single-negative materials," *Optik*, Vol. 121, 1558-1562, 2010.
- [34] Xiang, Y., X. Dai, S. Wen, and D. Fan, "Properties of omnidirectional gap and defect mode of one-dimensional photonic crystal containing indefinite metamaterials with a hyperbolic dispersion," *J. Appl. Phys.*, Vol. 102, 093107-093111, 2007.
- [35] Wang, H., Y. Luo, Y.T. Wang, H.B. Zhang, and Y.T. Fang, "Splitting of defect-mode in one-dimensional

- magnetic photonic crystal,” *Physica B*, Vol. 406, 2977-2981, 2012.
- [36] Born, M. and E. Wolf, *Principles of Optics: Electromagnetic theory of propagation, Interference and diffraction of light*, Cambridge University Press, UK, 2005.
- [37] Zhang, L., Y. Zhang, L. He, Z. Wang, H. Li, and H. Chen, “Zero- \bar{n} gaps of photonic crystals consisting of positive and negative index materials in microstrip transmission lines,” *J. Phys. D: Appl. Phys.*, Vol. 40, 2579-2587, 2007.
- [38] Li, J., L. Zhou, C.T. Chan, and P. Sheng, “Photonic band gap from a stack of positive and negative index materials,” *Phys. Rev. Lett.*, Vol. 90, 083901-083904, 2003.
- [39] Aghajamali, A. and M. Barati, “Effects of normal and oblique incidence on zero- \bar{n} gap in periodic lossy multilayer containing double-negative materials,” *Physica B*, Vol. 407, 1287-1291, 2012.
- [40] Yeh, P., *Optical waves in layered media*, Wiley Series in Pure and Applied Optics, 1988.
- [41] Daninthe, H., S. Foteinopoulou, C.M. Soukoulis, “Omni-reflectance and enhanced resonant tunneling from multilayers containing left-handed materials,” *Photon. Nanostruct.*, Vol. 4, 123-131, 2006.
- [42] Awasthi, S.K., A. Mishra, U. Malaviya, and S.P. Ojha, “Wave propagation in a one-dimensional photonic crystal with metamaterial,” *Solid State Commun.*, Vol. 149, 1379-1383, 2009.

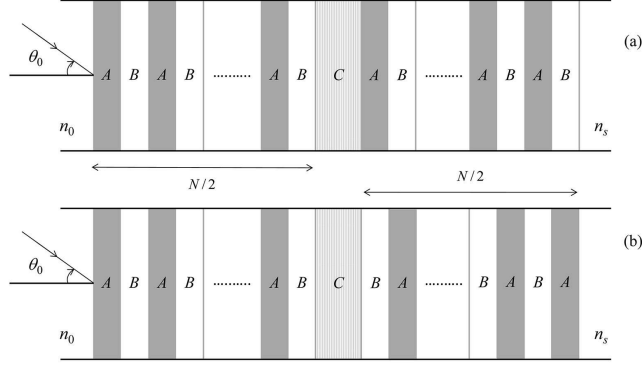


FIG. 1: Schematic diagrams of 1D defective MPCs embedded in air, with a defect layer, (a) asymmetric structure, (b) symmetric structure, where layers A and C are NIMs and layer B is PIM. The number of the periods is N and the incidence angle is θ_0 .

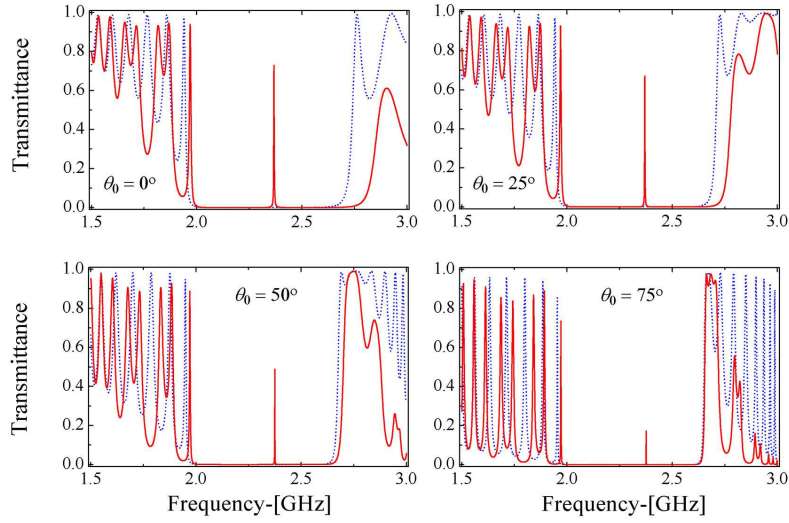


FIG. 2: Transmission spectra of TE polarized wave for the asymmetric 1D MPC structures with type-I NIM defect layer (solid line) and without defect layer (dotted line) for different incidence angles with $\gamma = 0.2 \times 10^{-3}$ GHz.

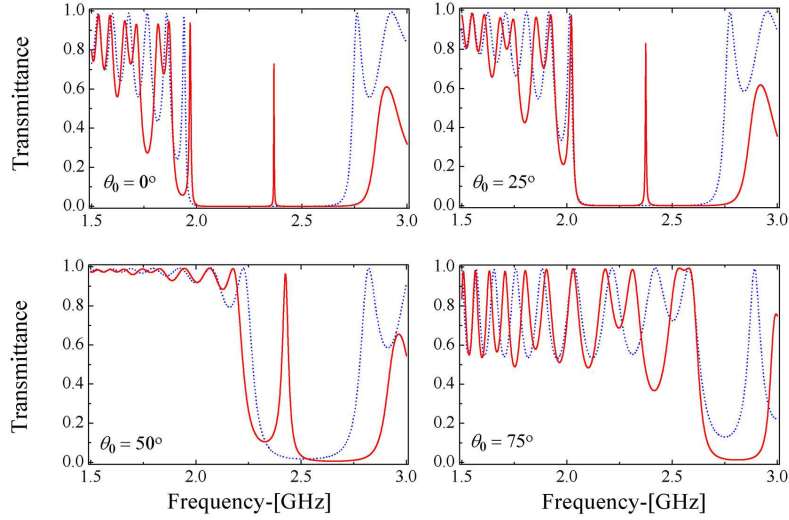


FIG. 3: Transmission spectra of TM polarized wave for the asymmetric 1D MPC structures with type-I NIM defect layer (solid line) and without defect layer (dotted line) for different incidence angles with $\gamma = 0.2 \times 10^{-3}$ GHz.

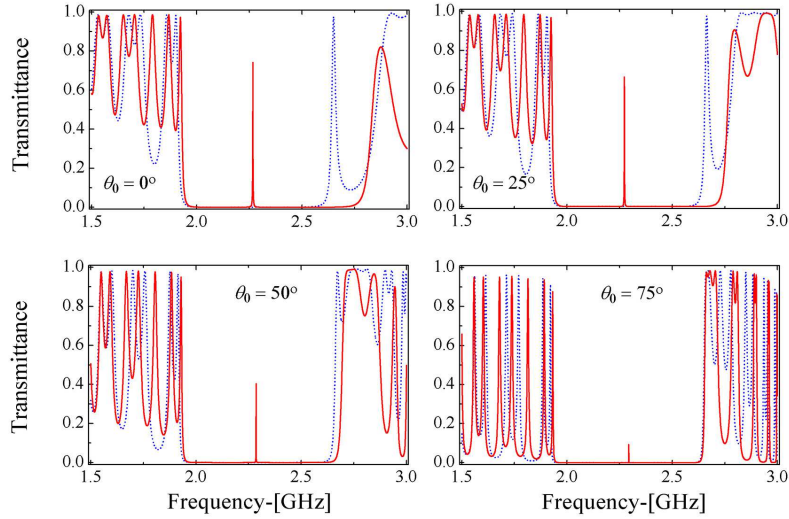


FIG. 4: Transmission spectra of TE polarized wave for the symmetric 1D MPC structures with type-I NIM defect layer (solid line) and without defect layer (dotted line) for different incidence angles with $\gamma = 0.2 \times 10^{-3}$ GHz.

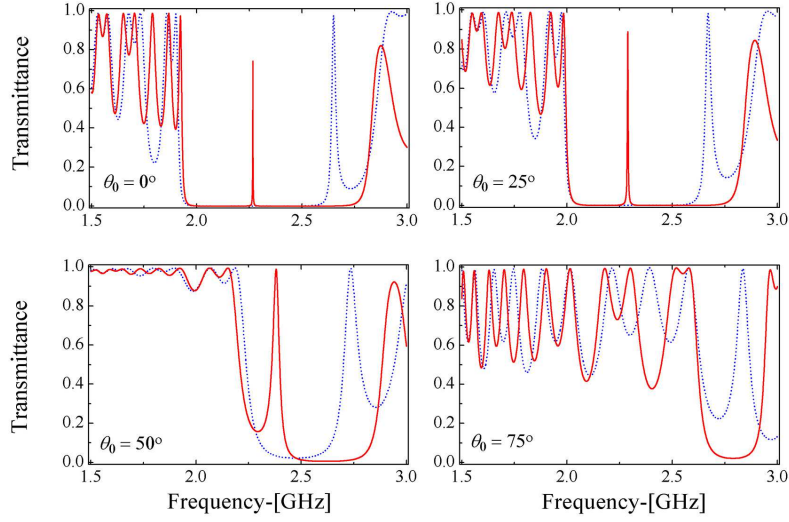


FIG. 5: Transmission spectra of TM polarized wave for the symmetric 1D MPC structures with type-I NIM defect layer (solid line) and without defect layer (dotted line) for different incidence angles with $\gamma = 0.2 \times 10^{-3}$ GHz.

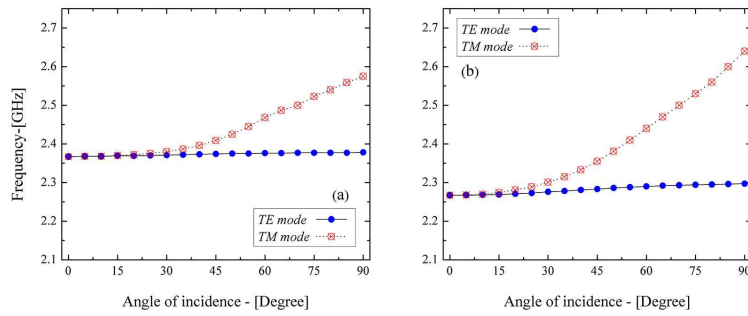


FIG. 6: Frequency of the defect modes in (a) the asymmetric and (b) the symmetric 1D PMCs as a function of angle of incidence for both polarizations, with $\gamma = 0.2 \times 10^{-3}$ GHz.

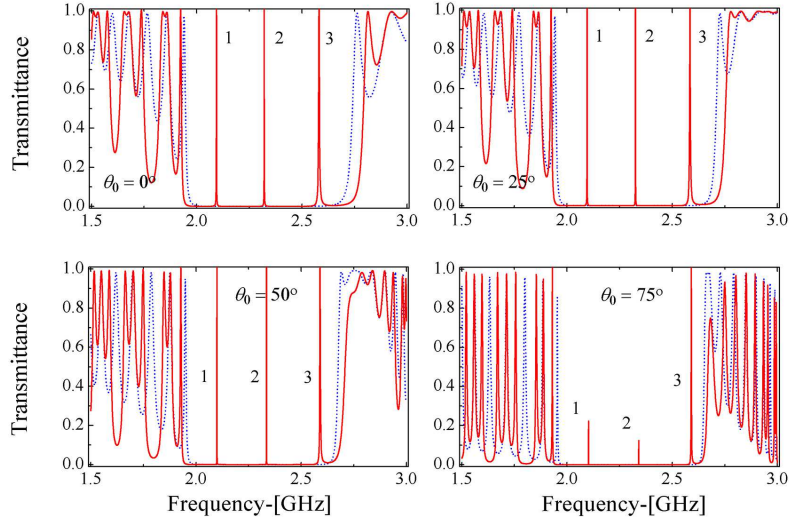


FIG. 7: Transmission spectra of TE polarized wave for the asymmetric 1D MPC structures with type-II NIM defect layer (solid line) and without defect layer (dotted line) for different incidence angles with $\gamma = 0.2 \times 10^{-3}$ GHz.

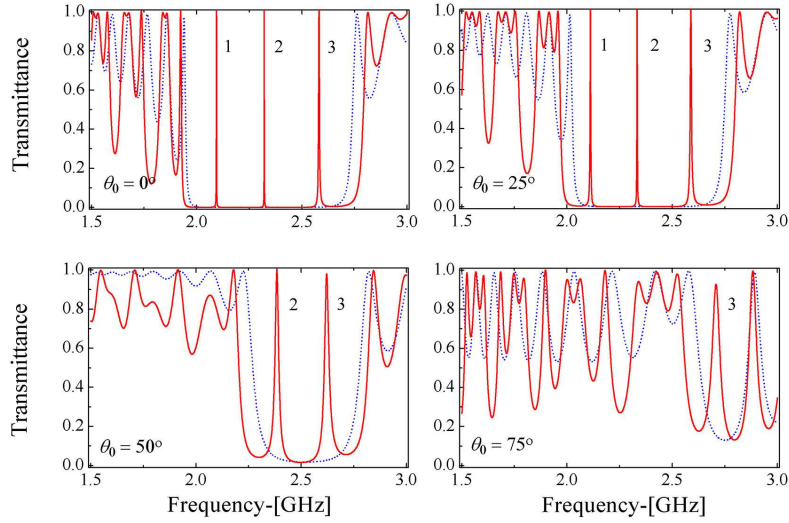


FIG. 8: Transmission spectra of TM polarized wave for the asymmetric 1D MPC structures with type-II NIM defect layer (solid line) and without defect layer (dotted line) for different incidence angles with $\gamma = 0.2 \times 10^{-3}$ GHz.

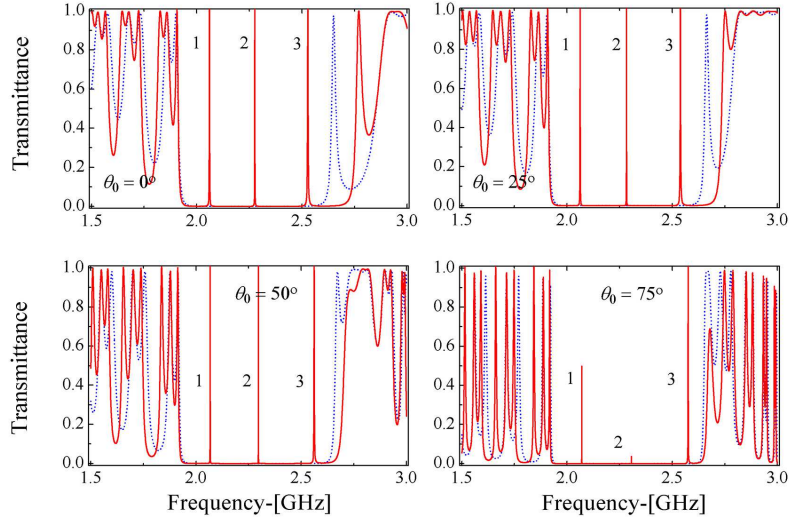


FIG. 9: Transmission spectra of TE polarized wave for the symmetric 1D MPC structures with type-II NIM defect layer (solid line) and without defect layer (dotted line) for different incidence angles with $\gamma = 0.2 \times 10^{-3}$ GHz.

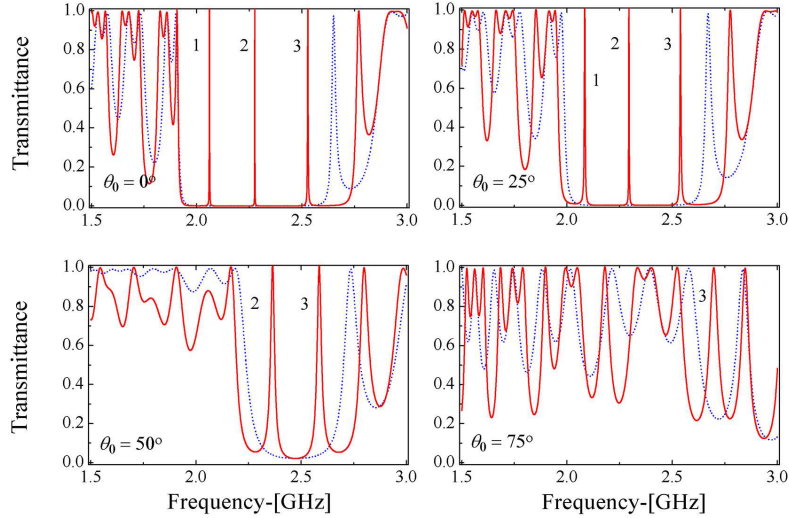


FIG. 10: Transmission spectra of TM polarized wave for the symmetric 1D MPC structures with type-II NIM defect layer (solid line) and without defect layer (dotted line) for different incidence angles with $\gamma = 0.2 \times 10^{-3}$ GHz.

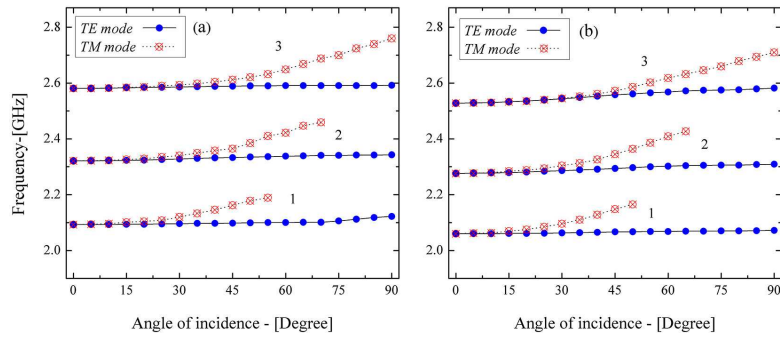


FIG. 11: Frequency of the defect modes in (a) the asymmetric and (b) the symmetric 1D PMCs as a function of angle of incidence for both polarizations, with $\gamma = 0.2 \times 10^{-3}$ GHz.